HYDROTHERMAL SYNTHESIS OF ZnO POWDERS WITH A TAILORED PARTICLE MORPHOLOGY AND IMPROVED OPTICAL CHARACTERISTICS

A. Stanković[1], Z. Stojanović[1], Lj. Veselinović[1], I. Bračko[2], S. Škapin[2], S. Marković[1] and D. Uskoković[1]

[1] Centre for Fine Particles Processing and Nanotechnologies, Institute of Technical Sciences of SASA, Belgrade, Serbia
[2] Jožef Štefan Institute, Ljubljana, Slovenia

Abstract

In order to investigate the effect of particle size and morphology on the optical properties of ZnO, a series of ZnO powders were synthesized by low-temperature hydrothermal processing using zinc acetate dihydrate and sodium hydroxide as the starting materials, and polyvinylpyrrolidone as the stabilizing agent. The particle size and morphology were tailored by adjusting the reactant molar ratios $[Zn^{2+}]/[OH^-]$, while the reaction temperature and time remained unchanged. XRD, TEM, SAED and HRTEM analyses have shown that the powders have a high crystalline pure wurtzite structure with nanosized crystallites. The size and morphology of the ZnO powders were investigated by FE-SEM, which showed a modification from micro-rods *via* hexagonal-faceted prismatic morphology to nano-spheres, by simple adjusting of the reactant molar ratios $[Zn^{2+}]/[OH^-]$ from 1:1 to 1:5. The optical properties of the ZnO powders as well as their dependence on the particle size and morphology were investigated by Raman and UV-Vis diffuse reflectance spectroscopy (DRS).

Experimental

In the series of experiments, the reaction temperature and time were kept constant, while the $[Zn^{2+}]/[OH^-]$ molar ratio in the starting solution was changed in order to tailor the particle size and shape. Namely, the $[Zn^{2+}]/[OH^-]$ molar ratio was varied from 1:1, 1:2, 1:3, 1:3.5, 1:4 to 1:5, resulting in the pH values of the reaction solution: 8, 9, 10, 11, 12 and 13, respectively. The starting materials, zinc acetate dihydrate ($Zn(CH_3COO)_2{\cdot}2H_2O$), sodium hydroxide (NaOH) and polyvinylpyrrolidone (PVP, $(C_6H_9NO)n$) as a stabilizing agent, were used without any additional treatment. (0.01 mol) of zinc acetate dihydrate and 0.0574 g (2·10-6 mol, i.e. 5 wt%) of PVP were dissolved in 750 ml of deionized water with a constant stirring at 1000 rpm and heating at 80 C. After the dissolution of zinc acetate dihydrate and PVP, an adequate amount of the aqueous solution of NaOH was added dropwise, resulting in a white precipitate. The as-prepared suspension was thermally treated in 2 l *Parr* stainless steel stirred reactor under non-equilibrium conditions up to 120 C at a constant heating rate of 2 C/min, under constant stirring of 400 rpm. The reaction time was 72 h.

Results and discussion

The XRD patterns of the prepared ZnO powders are presented in Fig. 1. All of the diffraction peaks in the recorded XRD patterns are in agreement with those of hexagonal wurtzite ZnO without peaks related to impurities or ZnO in other crystal phases. The unit cell parameters, crystallite size (D) in crystallographic directions [100], [010] and [002], and the crystallinity degree of the ZnO powders are calculated and listed in Table 1.

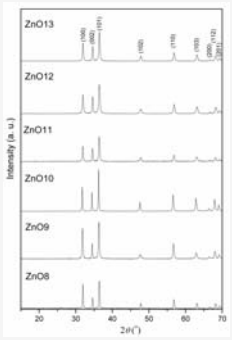

Fig. 1. XRD patterns of ZnO powders with different morphologies.

Sample	pH	Concentration [M]			Crystallinity degree X_c [%]	Crystallite size D, [nm]			Unit cell parameters [Å]	FE-SEM particles morphology (Fig. 2)
		$[Zn^{2+}]$	$[OH^-]$	[PVP]		[100]	[010]	[002]		
ZnO8	8	0.01	0.01	2·10⁻⁶	80.0	45	36	35	a=b=3.2465 c=5.2030	Micro-rods
ZnO9	9		0.02		81.0	38	28	30	a=b=3.2481 c=5.2062	Non-ordered hexagonal prism rods
ZnO10	10		0.03		91.0	40	34	38	a=b=3.2464 c=5.2019	Ordered hexagonal prism rods
ZnO11	11		0.035		80.0	33	27	29	a=b=3.2431 c=5.1985	Ellipsoids
ZnO12	12		0.04		88.0	27	22	24	a=b=3.2409 c=5.1940	Spheroids
ZnO13	13		0.05		93.0	30	40	35	a=b=3.2420 c=5.1971	Nano-spheres

Table. 1. Synthesis conditions and characteristics of prepared ZnO powders.

Fig. 8 shows the room temperature μ-Raman spectra of the synthesized ZnO powders. The modes that appear in the Raman spectra and can be assigned to the wurtzite crystal structure are the following: the most intensive band is E2L near 100 cm^{-1}, attributed to the vibrations of the zinc sublattice in ZnO the bands near 200, 320 and 380 cm^{-1} are attributed to 2E2L, the second-order acoustic mode E2H-E2L and A1 (TO), respectively. All of the spectra contain a sharp, strong and dominant peak located at about 440 cm^{-1}, which is the characteristic scattering peak of the Raman-active dominant E2H mode of wurtzite hexagonal ZnO and is assigned to oxygen vibration.

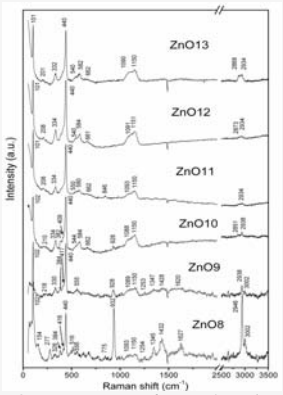

Fig. 8. Raman spectra of ZnO powders with different morphologies.

Assignment			Raman shift (cm^{-1})						
ZnO	PVP	defects	ZnO8	ZnO9	ZnO10	ZnO11	ZnO12	ZnO13
E_{2L}		✓	100 154	102	102	101	101	101
$2E_{2L}$		✓	277 326	218 330	210 334	209 334	208 334	201 332
E_{1H}-E_{2L} A_1 (TO)			384 416	384 417	382 409			
E_{2H}			440	440	440	440	440	440
		Si	516					
		A_1 (LO) + E_1 (LO)	556 625, 678	555 664	544, 584 662	550, 583 662	540, 584 661	540, 582 662
	C-N stretching	✓	775					
	C-C stretching	✓	847 932	928	928	946		
2LO A1 (2LO)			1093 1150	1089 1150	1088 1150	1093 1150	1091 1151	1090 1150
	C-N stretching		1254	1253				
A_2 (TO)-A_2(LO)+E^2_{2H}	C-H bending		1345 1432	1347 1428				
	C-O		1627	1620				
	C-H stretching		2944	2938		2851, 2938	2934	2873, 2934	2868, 2934
		Zn-OH	3002	3002				

Table. 2. Assignment and positions (wavenumber in cm^{-1}) of Raman bands in the spectra of ZnO powders.

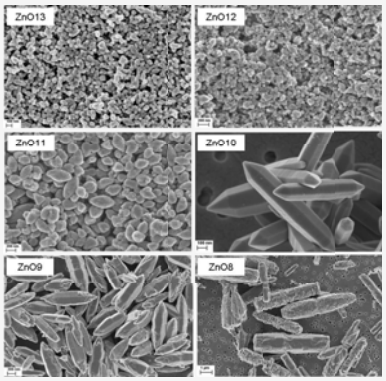

Fig. 2. The morphologies of the synthesized ZnO powders.

Fig. 3a shows a low-magnification TEM image of the ZnO hexagonal micro-rods synthesized at pH 10. The SAED pattern, Fig. 3b, performed along the [010] zone axis, indicates that the micro-rods are single crystalline in nature and the maxima can be indexed as the hexagonal $P6_3mc$ space group typical of the wurtzite crystal structure. Fig. 4a shows the TEM image of a ZnO particle synthesized at pH 11. The SAED pattern, Fig. 4b, composed of bright spots, indicates that the ellipsoidal ZnO particle is single crystalline; the estimated diffraction maxima correspond to the highly crystalline and hexagonal phase. Fig. 5a shows a TEM image of the ZnO particles synthesized at pH 13. The SAED pattern, Fig. 5b, proves that ZnO13 has high crystallinity and a hexagonal wurtzite crystal structure. According to the HRTEM images of the analyzed samples, Figs. 3c, 4c and 5c, there are no detectable traces of secondary phases, defects or clusters.

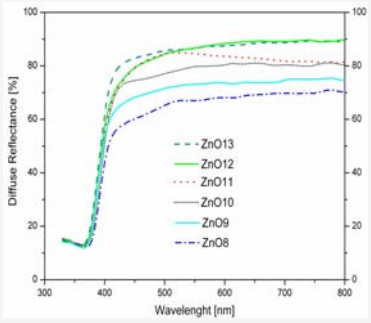

Fig. 6. Kubelka-Munk curves for the ZnO powders with different morphologies.

Diffuse reflectance spectra of ZnO powders with different size and morphology, Fig. 6, revealed characteristic R curves with the absorption edge near 380 nm. The micro-sized powder ZnO8 revealed the lowest reflectance (~70%), compared to submicro- (~80%) and nano-sized (ZnO12 and ZnO13, ~90%) powders. Influence of the particle size and morphology on the absorption of visible light is evidenced by the shift of the absorption curves to larger wavelenghts (red shift) and by the enhancement of Urbach tails. The Kubelka-Munk relation was used to convert the diffuse reflectance spectra R into the equivalent absorption spectra F.

The morphologies of the synthesized ZnO powders are shown in Fig. 2. ZnO8 powder, synthesized at pH 8, consists of micro-rods The hydrothermal processing performed at pH 9 led to changes in the particle shape from cracked micro-rods to non-ideal hexagonal prisms; the edges of the hexagonal prisms were non-ordered, while the pyramids at their ends were partly formed. At pH 10, the particles with regular geometrical shape corresponding to the hexagonal structure and uniform size distribution were prepared (Fig. 2, ZnO10). Powder ZnO11, consists of ellipsoidal particles. When the pH value was tuned to 12, powder with spherical particles which tend to group in clusters of around 200 nm in diameter was synthesized, ZnO12. Finally, ZnO13 powder, synthesized at pH 13 consists of spherical nano-sized particles with average diameters of ~ 50 nm.

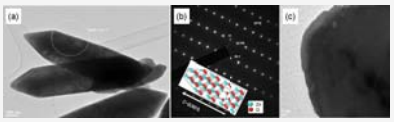

Fig. 3. (a) A low-magnification TEM image, (b) SAED pattern and (c) HRTEM image of ZnO10 powder.

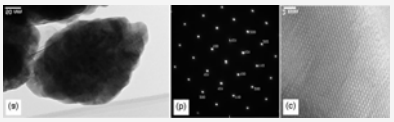

Fig. 4. (a) A low-magnification TEM image, (b) SAED pattern and (c) HRTEM image of ZnO11 powder.

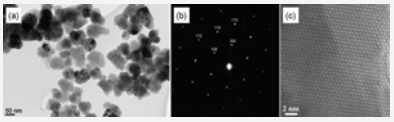

Fig. 5. (a) A low-magnification TEM image, (b) SAED pattern and (c) HRTEM image of ZnO13 powder.

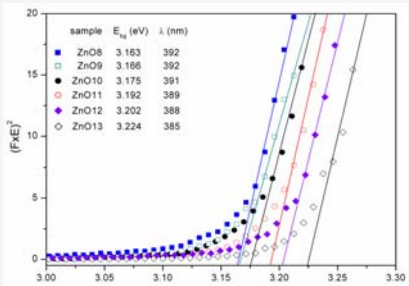

Fig. 7. Diffuse reflectance spectra of ZnO powders with different morphologies.

The direct band gap energies (Ebg) of the ZnO powders were determined by the extrapolation of the linear part of the absorption function (FxE)2, presented in Fig. 7. A slight red-shift of 0.06 eV which occurs in the absorption edge, meaning that micro-rods absorb a larger amount of visible light, can be explained by a longer optical path for light transport through the micro-rods (ZnO8, ZnO9) than through sub-micro or nano-particles (ZnO10-ZnO13) resulting in a greater a a greater absorption capacity.